

## Propolin H from Taiwanese Propolis Induces G1 Arrest in Human Lung Carcinoma Cells

MENG-SHIH WENG,<sup>†</sup> CHIUNG-HO LIAO,<sup>†</sup> CHIA-NAN CHEN,<sup>†</sup> CHIA-LI WU,<sup>‡</sup> AND JEN-KUN LIN<sup>\*,†</sup>

Graduate Institute of Biochemistry and Molecular Biology, College of Medicine, National Taiwan University, Taipei 10018, Taiwan, and Department of Chemistry, Tamkang University, Tamsui 251, Taiwan

Propolis, a natural product collected by honeybee, has been reported to exert a wide spectrum of biological functions. In this study, we have isolated a novel component, namely, propolin H, and investigated its effects in human carcinoma cells. Propolin H inhibited the proliferation of human lung carcinoma cell lines in MTT assay, and a significant G1 arrest was observed to occur in a dose-dependent manner at 24 h of exposure in H460 cells. After treatment with propolin H in H460 cells, the content of the CDK inhibitor p21<sup>Waf1/Cip1</sup> protein increased in correlation with the elevation in p53 levels. Western blot analysis of G1 regulatory proteins further revealed a decrease in cyclin-dependent kinase 2 (CDK2) and CDK4 and an increase in cyclin E. The CDKs kinase activities assay showed that propolin H has inhibited CDK2 and CDK4 kinase activities. Accordingly, coimmunoprecipitations revealed an increased association of both CDK2 and CDK4 immunoreactive protein with the p21<sup>Waf1/Cip1</sup> protein complex under propolin H-treated conditions. Additionally, we found that propolin H enhanced the expression of p21<sup>Waf1/Cip1</sup> in p53-mutant and p53-null lung carcinoma cell lines, following the induction of G1 arrest. Together, these findings suggest that the induction of p21<sup>Waf1/Cip1</sup> expression occurred through p53-dependent and -independent pathways in propolin H-treated cells. Propolin H exerts its significantly growth inhibitory effects and may have therapeutic applications.

**KEYWORDS:** Propolis; propolin H; lung carcinoma cell; cell cycle; p21<sup>Waf1/Cip1</sup>

### INTRODUCTION

The proliferation of mammalian cells is normally determined by extracellular signals that engage a program of gene expression and protein regulation required for cell division (1, 2). The first gap phase (G1) and initiation of DNA synthesis (S) during the cell division cycle are cooperatively regulated by several key molecules, including cyclin-dependent kinases (CDKs) and their inhibitors (CDKIs) (3–5). Several checkpoints control a signaling system that changes the activity of CDKs, monitoring DNA damage and delaying cell cycle progression (2, 6). Two major pathways involved in the cellular progression from the G<sub>0</sub> to the S phase include the Rb (Rb, cyclin D1, and p16<sup>INK4A</sup>) cell cycle pathway and the p53/p21<sup>Waf1/Cip1</sup> G<sub>1</sub>–S checkpoint arrest pathway (7–10). p21<sup>Waf1/Cip1</sup>, one of the CDK inhibitors, was identified as a p53-responsive gene, and it plays a critical role in p53-induced G1 arrest (11).

Propolis is a resinous substance collected by honeybees from various plant sources, and it is used in the construction and maintenance of their hives (12). Propolis is alleged to possess a broad spectrum of biological activities, including antioxidant,

antibiotic, antiviral, and anti-inflammatory activities (13–17). The largest constituents of propolis are defined as terpenes, various phenylpropane derivatives such as caffeic acid esters, flavonoids, amino acids, or a large number of aldehydes and ketones (18–20). We previously isolated six novel prenylflavanones from Taiwan propolis, named propolins A, B, C, D, E, and F (Figure 1) (21–23). Propolins A and B have hydrated geranyl side chains, and propolin C has an unhydrated geranyl side chain. Our studies indicated that propolin C induced apoptosis through a mitochondria-dependent pathway, and propolin C was more effective in inducing apoptosis than either propolin A or B in human melanoma cells. Moreover, propolin C is a potential antioxidant agent and shows a strong capability to scavenge free radicals and inhibit xanthine oxidase activity (21, 22, 24).

In this study, a new component, propolin H, was identified, and its biological activities were characterized. The modulation effects associated with p53 that regulate the cell cycle were investigated. Our data suggested that propolin H could be beneficial in chemoprevention.

### MATERIALS AND METHODS

**Propolin H Isolated from the Taiwanese Propolis.** Taiwanese propolis glue (245 g, mixture from hives collected near Bagwa Shan,

\* To whom correspondence should be addressed. Tel: 886-2-2356-2213. Fax: 886-2-2391-8944. E-mail: jklin@ha.mc.ntu.edu.tw.

<sup>†</sup> National Taiwan University.

<sup>‡</sup> Tamkang University.

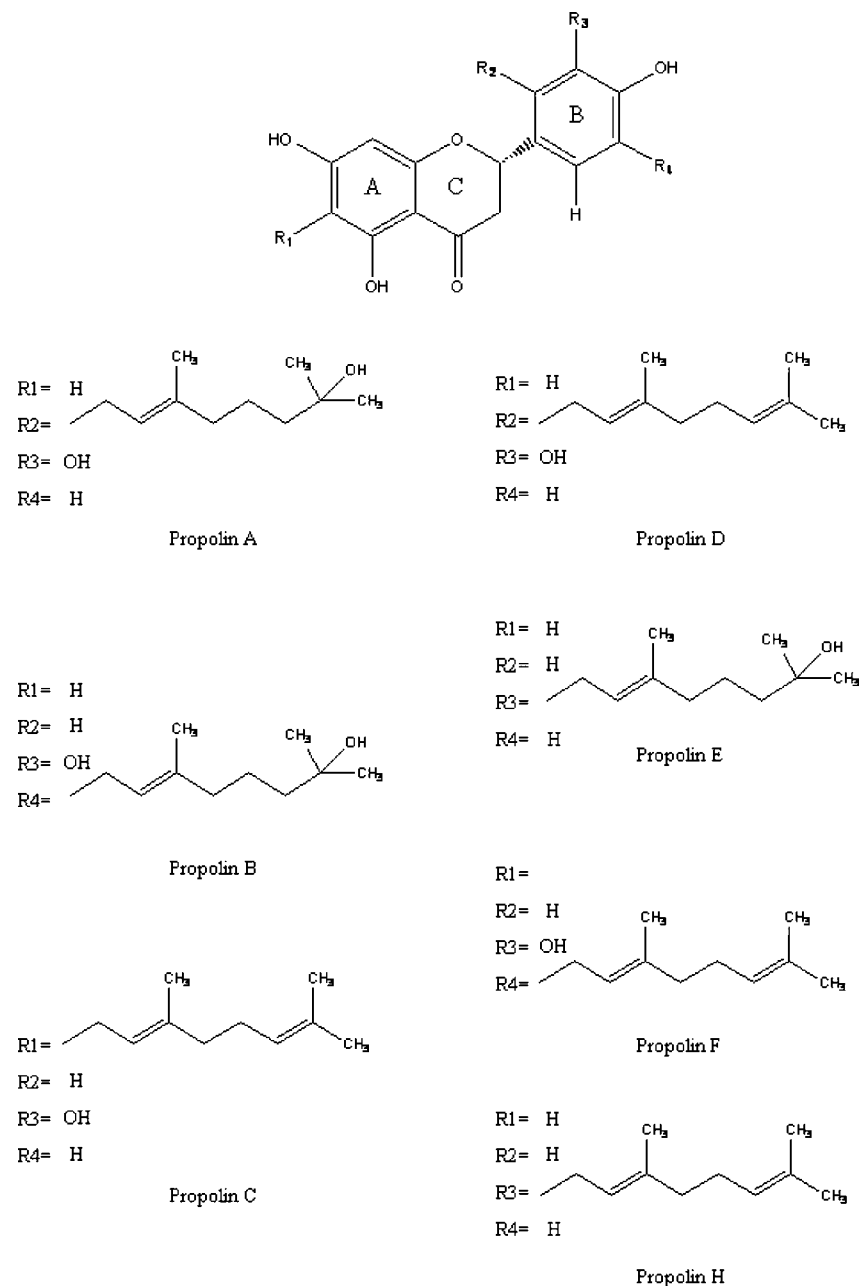


**Figure 1.** Structures of propolins.

Taiwan) was homogenized by stirring at 4 °C and was washed three times with 0.7 L of deionized water. The residue was extracted three times with 95% ethanol. The filtered ethanol extract was evaporated to dryness under reduced pressure to furnish a brown powder, which was kept at -20 °C until further purification. The brown powder from the ethanol extract was dissolved in methanol and applied to a Sephadex LH-20 column (Amersham Pharmacia Biotech AB) using 95% ethanol as the eluting solvent. All eluates, including fractions from the follow-up chromatographies, were assayed on human melanoma proliferation, and the active fractions were again chromatographed on Sephadex LH-20 column using 95% ethanol to elute. The active fractions were subjected to silica gel column chromatography (Kiesel gel, E. Merck) using a solvent system of *n*-hexane-EtOAc. Purification of the most active fraction (*n*-hexane-EtOAc = 40:60) was carried out on a reverse-phase preparative high-performance liquid chromatography (HPLC). Fractions of retention times at 28 min containing propolin H were collected. The conditions were as follows: column-Luna Phenomenex, C18, 250 mm × 10 mm (United States); solvent system, methanol:water (8:2); flow rate, 3 mL/min; and detection, UV 280 nm. Propolin H was obtained as a slightly yellow powder from the eluate of 80%

methanol/water. The <sup>1</sup>H and <sup>13</sup>C NMR data of propolin H are compiled in **Tables 1** and **2**.

**Cell Culture and Cytotoxicity Assay.** Human nonsmall cell lung cancer (NSCLC) p53 wild-type H460, p53-mutant H1155, and p53-null H1299 cell lines were obtained from the American Type Culture Collection (Manassas, VA) and cultured in RPMI-1640 medium (Hyclone Laboratories, Logan, UT) supplemented with 10% fetal calf serum (FCS, Hyclone Laboratories) and 100 U of penicillin-streptomycin. Cells were maintained at 37 °C in a humidified atmosphere at 95% air and 5% CO<sub>2</sub>. All cells (1 × 10<sup>4</sup>) per well were cultured in 96 well plates. After incubation for 24 h, cells were washed and treated with different concentrations of propolin H in each well in triplicate for 24 h. Cell viability was determined by the MTT assay.

**Cell Synchronization, Drug Treatment, and Flow Cytometric Cell Analysis.** After 24 h of plating of the cells, the medium was removed. Cells were washed three times with phosphate-buffered saline (PBS) and then incubated with serum-free medium for 24 h. Under these conditions, cells were arrested in the G0/G1 phase, as determined by flow cytometry analysis. The serum-free medium was removed and changed to the fresh medium containing 10% FCS. Propolin H or E

**Table 1.**  $^1\text{H}$  NMR Data of Propolin H and Propolin E<sup>a</sup> in  $\text{CDCl}_3$ <sup>b</sup>

position	propolin H $\delta_{\text{H}}$ (J, Hz)	position	propolin E $\delta_{\text{H}}$ (J, Hz)
2 $\beta$	CH 5.30 (dd, 12.8, 2.9)	2 $\beta$	CH 5.20 (dd, 11.6, 3.0)
3 $\beta$	CH <sub>2</sub> 2.67 (dd, 17.1, 3.1)	3 $\beta$	CH <sub>2</sub> 2.60 (dd, 17.1, 3.0)
3 $\alpha$	3.10 (dd, 17.1, 12.8)	3 $\alpha$	3.10 (dd, 17.1, 11.6)
6	CH 5.86 (d, 2.1)	6	CH 5.86 (d, 2.0)
8	CH 5.88 (d, 2.1)	8	CH 5.88 (d, 2.0)
2'	CH 7.15 (d, 2.0)	2'	CH 7.16 (d, 2.1)
5'	CH 6.77 (d, 8.2)	5'	CH 6.77 (d, 8.2)
6'	CH 7.11 (dd, 8.3, 2.2)	6'	CH 7.10 (dd, 8.2, 2.1)
1''	CH <sub>2</sub> 3.34 (d, 7.0)	1''	CH <sub>2</sub> 3.32 (d, 6.6)
2''	CH 5.31 (t, 7.0)	2''	CH 5.3
4''	CH <sub>3</sub> 1.69 (s)	4''	CH <sub>3</sub> 1.69 (s)
5''	CH <sub>2</sub> 2.03 (t, 7.3)	5''	CH <sub>2</sub> 2.03 (t, 6.8)
6''	CH <sub>2</sub> 2.10 (m)	6''	CH <sub>2</sub> 1.50 (m)
7''	CH 5.10 (t, 7.3)	7''	CH <sub>2</sub> 1.40 (t, 6.8)
9''	CH <sub>3</sub> 1.55 (s)	9''	CH <sub>3</sub> 1.13 (s)
10''	CH <sub>3</sub> 1.61 (s)	10''	CH <sub>3</sub> 1.13 (s)

<sup>a</sup> Data taken from ref 23. <sup>b</sup> Assignments were based on the HMQC and HMBC NMR data.

**Table 2.**  $^{13}\text{C}$  NMR Data of Propolin H and Propolin E<sup>a</sup>

carbon no.	propolin H in $\text{CDCl}_3$ $\delta_{\text{C}}$	propolin E in $\text{CDCl}_3$ $\delta_{\text{C}}$
2	80.7	80.6
3	44	44.2
4	197.8	197.8
5	164.9	164.8
6	97	97
7	168.4	168.4
8	96.2	96.2
9	165.4	165.2
10	103.3	103.4
1'	130.8	130.9
2'	128.9	128.9
3'	129.5	129.5
4'	156.7	156.7
5'	115.9	119.5
6'	126.2	126.3
1''	29.1	29.1
2''	123.7	123.7
3''	137	137.2
4''	16.2	16.1
5''	40.9	41.2
6''	27.7	23.7
7''	125.3	44.3
8''	132.2	71.5
9''	17.8	29.2
10''	25.9	29.1

<sup>a</sup> Data taken from ref 23. Assignments were also based on the HMQC and HMBC NMR data obtained, respectively.

solutions were prepared by dissolving this compound in a final concentration of 0.1% (v/v) dimethyl sulfoxide (DMSO). The cell cycle progression was measured by flow cytometry analysis.

**Western Blot Analysis.** Treated and untreated cells were rinsed twice with ice-cold PBS and then lysed in an appropriate extraction buffer (10 mM Tris-HCl, pH 7; 140 mM sodium chloride; 3 mM magnesium chloride; 0.5% [v/v] NP-40; 2 mM phenylmethylsulfonyl fluoride; 1% [w/v] aprotinin; and 5 mM dithiothreitol) for 30 min on ice. The extracts were centrifuged for 30 min at 12000g. Proteins were loaded at 50  $\mu\text{g}$ /lane on sodium dodecyl sulfate (SDS)-polyacrylamide gel and then transferred to nitrocellulose membranes. The membranes were blocked for 30 min at room temperature in PBS plus 0.5% Tween 20 containing 1% bovine serum albumin and then incubated for 2 h at room temperature with 1:1000 dilution of one of the mouse monoclonal antibodies against human cyclin D1, CDK2, p21 (1:1000 dilution, Santa Cruz, CA), p21 or  $\beta$ -actin (1:1000 dilution, Transduction Laboratories, KY), or rabbit polyclonal anti-human CDK4, cyclin E (1:1000 dilution), and p53 (1:1000 dilution, Transduction Laboratories) antibody. After

washing, the membranes were incubated for 60 min at 25 °C with the 1:3000 dilution of appropriate horseradish peroxidase-labeled secondary antibody, and bound antibody was visualized and quantified by chemiluminescence detection (Amersham, IL). Actin was used as the internal control. The amount of the protein of interest, expressed as arbitrary densitometric units, was normalized to the densitometric units of actin. The density of the band was then expressed as the relative density as compared to that in untreated cells (control), which was taken as one-fold.

**Immunoprecipitation and CDKs Kinase Assay.** For the CDK kinase assay, lung cancer cells H460 ( $3 \times 10^5$ /dish) were precultured in 100 mm culture dishes for 24 h and then starved for 24 h. After starvation, cells were changed to fresh, complete medium and treated with 0 or 40  $\mu\text{M}$  propolin H for 24 h. After 24 h of propolin H treatment, H460 cells were rinsed twice with ice-cold PBS and lysed with Gold lysis buffer (10% glycerol, 1% Triton X-100, 1 mM sodium orthovanadate, 1 mM EGTA, 5 mM EDTA, 10 mM NaF, 1 mM sodium pyrophosphate, 20 mM Tris-HCl, pH 7.9, 100  $\mu\text{M}$   $\beta$ -glycerophosphate, 137 mM NaCl, 1 mM PMSF, 10  $\mu\text{g}/\text{mL}$  aprotinin, and 10  $\mu\text{g}/\text{mL}$  leupeptin) for 30 min at 4 °C. The cell lysate was clarified by centrifugation at 12000g for 30 min at 4 °C. A total of 250  $\mu\text{g}$  of protein was incubated with anti-CDK2 or anti-CDK4 antibody and protein A/G plus agarose (Santa Cruz, CA) for 18 h at 4 °C. The immunoprecipitate was washed thrice with immunoprecipitate buffer (1% Triton X-100, 150 mM NaCl, 10 mM Tris, pH 7.4, 1 mM EDTA, 1 mM EGTA, 0.2 mM sodium vanadate, 0.2 mM PMSF, and 0.5% NP-40) and thrice with kinase buffer (50 mM HEPES, pH 7.4, 10 mM MgCl<sub>2</sub>, 2.5 mM EDTA, 10 mM  $\beta$ -glycerophosphate, 1 mM NaF, and 1 mM DTT for CDK4; 50 mM HEPES, pH 7.4, 10 mM MgCl<sub>2</sub>, 2.5 mM EDTA, and 1 mM DTT for CDK2).

For the immunoprecipitation western analysis, the CDK2 and CDK4 immunoprecipitates were resuspended in 25  $\mu\text{L}$  of lysis buffer, mixed with 5 $\times$  Laemmli's loading buffer, and separated by SDS-polyacrylamide gel electrophoresis (PAGE) and then transferred to nitrocellulose and blotted with anti-p21. In each case, blots were stripped and reprobed with the antibody used for immunoprecipitation.

For the kinase assay, the CDK2 and CDK4 immunoprecipitates were washed with one of two kinase buffers (50 mM HEPES, pH 7.4, 10 mM MgCl<sub>2</sub>, 2.5 mM EDTA, and 1 mM DTT for CDK2; the same buffer but with 10 mM  $\beta$ -glycerophosphate and 1 mM NaF for CDK4) thrice. The kinase reactions were carried out in a final volume of 40  $\mu\text{L}$  containing 2  $\mu\text{g}$  of histone H1 (Calbiochem, San Diego, CA) or 1  $\mu\text{g}$  of Gst-Rb (Santa Cruz), 20  $\mu\text{M}$  cold ATP, and 5  $\mu\text{Ci}$  [ $\text{r}^{32}\text{p}$ ] ATP (5000 Ci/mmol, Amersham) and incubated for 20 min at 25 °C. Each sample was mixed with 10  $\mu\text{L}$  of Laemmli's loading buffer to stop the reaction, heated for 10 min at 100 °C, and subjected to SDS-PAGE. The gels were dried, visualized by autoradiography, and quantified by densitometry (IS-1000 Digital Imaging System). The kinase activities in each treatment were normalized with the levels of immunoprecipitation loading control as the relative activities as compared to that in untreated cells (control), taken as 100%.

**Statistical Analysis.** The results were expressed as means  $\pm$  standard errors (SEs) calculated from the specified numbers of determination. Comparisons were subjected to one-way analysis of variance followed by Fisher's least significant difference test. Significance was accepted at  $p < 0.05$ .

## RESULTS

**Purification and Identification of Propolin H.** Propolin H (**Figure 1**) was isolated after repeated chromatographies of the 95% ethanol extract of the propolis glue under the guidance of human melanoma proliferation. Final purification of the active fraction was achieved by HPLC on a reversed-phase column. The total content of the active component, propolin H, was 1.8% of the propolis glue. Both  $^1\text{H}$  and  $^{13}\text{C}$  NMR (in  $\text{CD}_3\text{OD}$ , **Tables 1** and **2**) displayed absorptions characteristic of the prenylfavanone type, very similar to those of propolin E, the more polar component, and isolated from the same source (1.2%) (23). The high-resolution mass spectrometry of a pure sample of propolin

H indicated an  $[M]^+$  of 408 with the molecular composition  $C_{25}H_{28}O_6$ . The main structural differences of propolins H and E are a water molecule elimination in the geranyl side chain. Moreover, the geranyl substitution is also on the B ring at C-3, the same as that of propolin E, judging from the coupling patterns of the two aromatic rings ( $\delta_H$  5.86, d,  $J$  = 2.1 Hz; 5.88, d,  $J$  = 2.1 Hz; 6.77, d,  $J$  = 8.2 Hz; 7.15, d,  $J$  = 2.1 Hz; and 7.11, dd,  $J$  = 8.2, 2.1 Hz). Propolin H is a novel compound characterized from Taiwanese propolis. In **Tables 1** and **2**, a complete assignment of each proton and each carbon of propolins E and H in *d*-methanol is compiled on the basis of the two-dimensional NMR data [heteronuclear multiple quantum coherence (HMQC), heteronuclear multiple bond correlation (HMBC), and nuclear Overhauser enhancement spectroscopy) observed.

**Propolin H Inhibits Cell Proliferation and Induces G1 Phase Cell Cycle Arrest in Human H460 Lung Cancer Cells.** To investigate the growth inhibitory effect of propolin H in tumor cells, we first assessed the antiproliferation efficacy of propolin H on human H460 lung cancer cells. These cells were treated with 0–80  $\mu$ M propolin H in 0.1% DMSO for 24 h, and the cell viability was measured by MTT assay (**Figure 2A**). The inhibitory effect was obvious after 24 h of treatment of 20–80  $\mu$ M propolin H in these cells, and the cell viability of 20, 40, and 80  $\mu$ M propolin H-treated cultures fell by approximately 14.8, 13.2, and 20%, respectively. In contrast, propolin E has also decreased the proliferation of H460 cells in a dose-dependent manner. After 24 h of incubation, the cell viability of 5, 10, 20, 40, and 80  $\mu$ M propolin E-treated cultures fell by approximately 19.2, 22.1, 23.5, 31.4, and 39.0%, respectively. We also examined the growth inhibitory effect of propolins H and E on human A2058 melanoma cells (**Figure 2B**). Our data showed that both propolins H and E also inhibited cell proliferation of A2058 melanoma cells in a dose-dependent manner. After 24 h of treatment, the cell viability of 5, 10, 20, and 40  $\mu$ M propolin H-treated A2058 cells fell by approximately 3.7, 38.5, 59.4, and 76.8%, respectively. In propolin E-treated A2058 cells, the cell viability fell by approximately 2.8, 11.2, 30.7, 23.5, and 54.5% after treatment with various concentrations propolin E for 24 h (5, 10, 20, and 40  $\mu$ M, respectively). To examine the reversibility of the propolin H-induced growth inhibition, the H460 cells were treated with 0–80  $\mu$ M propolin H. After 24 h of treatment, propolin H was removed and replaced with fresh medium. **Figure 2C** suggested that the inhibitory effect of propolin H was irreversible and was sustained to 48 h.

To assess whether propolin H-induced cell growth inhibition is mediated via alterations in cell cycle progression, H460 cells were synchronized by serum-free medium for 24 h and then by serum-supplemented medium containing propolin H (0, 5, 10, 20, and 40  $\mu$ M). To evaluate the effect of propolin H on cell cycle phase distribution, flow cytometry analysis was performed. As shown in **Figure 2D**, propolin H induces a G1 phase cell cycle arrest in a dose-dependent manner. The percentage of cells in G1 phase increased 57.8% in control and 75.1% with 40  $\mu$ M treatment of propolin H. In contrast to propolin H, propolin E did not increase cell cycle arrest at the G1 phase in H460 cells (**Figure 2E**). Furthermore, treatment with 40  $\mu$ M propolin H sustained G1 arrest at time points ranging from 0 to 24 h in H460 cells. Propolin H caused a roughly 18% increase in G1 arrest at 40  $\mu$ M for 24 h in H460 cells (**Figure 2F**).

**Down-Regulation of Cyclin D, Cyclin E, and Associated CDK Protein Levels, and CDK2- and CDK4-Associated Kinase Activities in Propolin H-Treated H460 Lung Cancer Cells.** It is well-known that cyclin D, cyclin E, CDK2, and CDK4/6 cooperate to promote G1 phase progression (3–5). To examine whether propolin H regulated the expression levels of these proteins in the G1 phase, H460 cells were synchronized by serum-free medium for 24 h and then serum-supplemented medium containing 40  $\mu$ M propolin H for various time points (0, 3, 6, 12, 18, and 24 h). After cells were harvested, western blot analyses were done with anti-cyclin D1, E, CDK2, and CDK4 antibodies, respectively. As shown in **Figure 3A**, the protein levels of CDK2 and CDK4 fell following treatment with propolin H at the experimental time points. The protein levels of cyclin E decreased at time points ranging from 6 to 18 h with 40  $\mu$ M propolin H in H460 cells. However, cyclin E was up-regulated at the time points of 24 h in propolin H-treated H460 cells. Otherwise, the protein level of cyclin D1 has been found slightly different between DMSO- and propolin H-treated cells.

It is well-known that cyclin D, cyclin E, CDK2, and CDK4/6 cooperate to promote G1 phase progression. To further verify whether the propolin H-induced down-regulation of CDK2 and CDK4 was associated with the enzyme activities of various cyclin–CDK complexes, an *in vitro* kinase assay was performed. Histone H1 or Gst-Rb was used as a substrate in immunoprecipitation experiments performed with antibodies against CDK2 and CDK4, respectively. The H460 cells were synchronized by serum-free medium for 24 h and then serum-supplemented medium containing DMSO or 40  $\mu$ M propolin H for 24 h. Lysates from cells treated with propolin H (40  $\mu$ M) for 24 h showed a significant decrease in kinase activities (**Figure 3B**). Densitometric analysis showed that kinase activities of CDK2 and CDK4 were decreased about 40 and 50%, respectively, in propolin H-treated cells. A propolin H-mediated decrease of CDK2 and CDK4 protein levels was consistent with reduction in their kinase activities. These results suggested that propolin H may inhibit the G1–S transition-related CDKs kinase activities, which should contribute to G1 arrest.

**Effects of Propolin H on Protein Expression of CDK Inhibitors p21<sup>Waf1/Cip1</sup>, p27<sup>Kip1</sup>, and p53 in Human H460 Lung Cancer Cells.** Numerous studies have shown that CDK inhibitors (CDKIs) regulate the progression of cells in the G0/G1 phase and an induction of CDKIs causes a blockade of G1/S transition thereby resulting in cell cycle arrest (3, 5, 6, 8). To determine whether propolin H induces the expressions of CDKIs, we first examined the effects of propolin H on the expressions of p21<sup>Waf1/Cip1</sup> and p27<sup>Kip1</sup> protein in H460 cells. After treatment of propolin H with various time points, cells were harvested and western blot analyses were done with anti-p21<sup>Waf1/Cip1</sup> and p27<sup>Kip1</sup> antibodies, respectively. As shown in **Figure 4A**, the protein levels of p21<sup>Waf1/Cip1</sup> displayed a maximum increase at 18 h (2.1-fold) in propolin H-treated H460 cells. However, p27<sup>Kip1</sup> displayed a decrease after propolin H treated for 24 h. The increase of p21<sup>Waf1/Cip1</sup> protein has been reported to occur through either p53-dependent or p53-independent mechanisms. The p53/p21<sup>Waf1/Cip1</sup> signaling plays a critical role in regulating the G1–S transition in response to a variety of cellular stresses (6, 8). Therefore, we furthermore examined the effect of propolin H on the protein levels of p53 in H460 cells. Our data showed that the protein levels of p53 had been observed as 1.5-fold increases at 18 h and sustained for 24 h (**Figure 4A**) in propolin H-treated H460 cells.

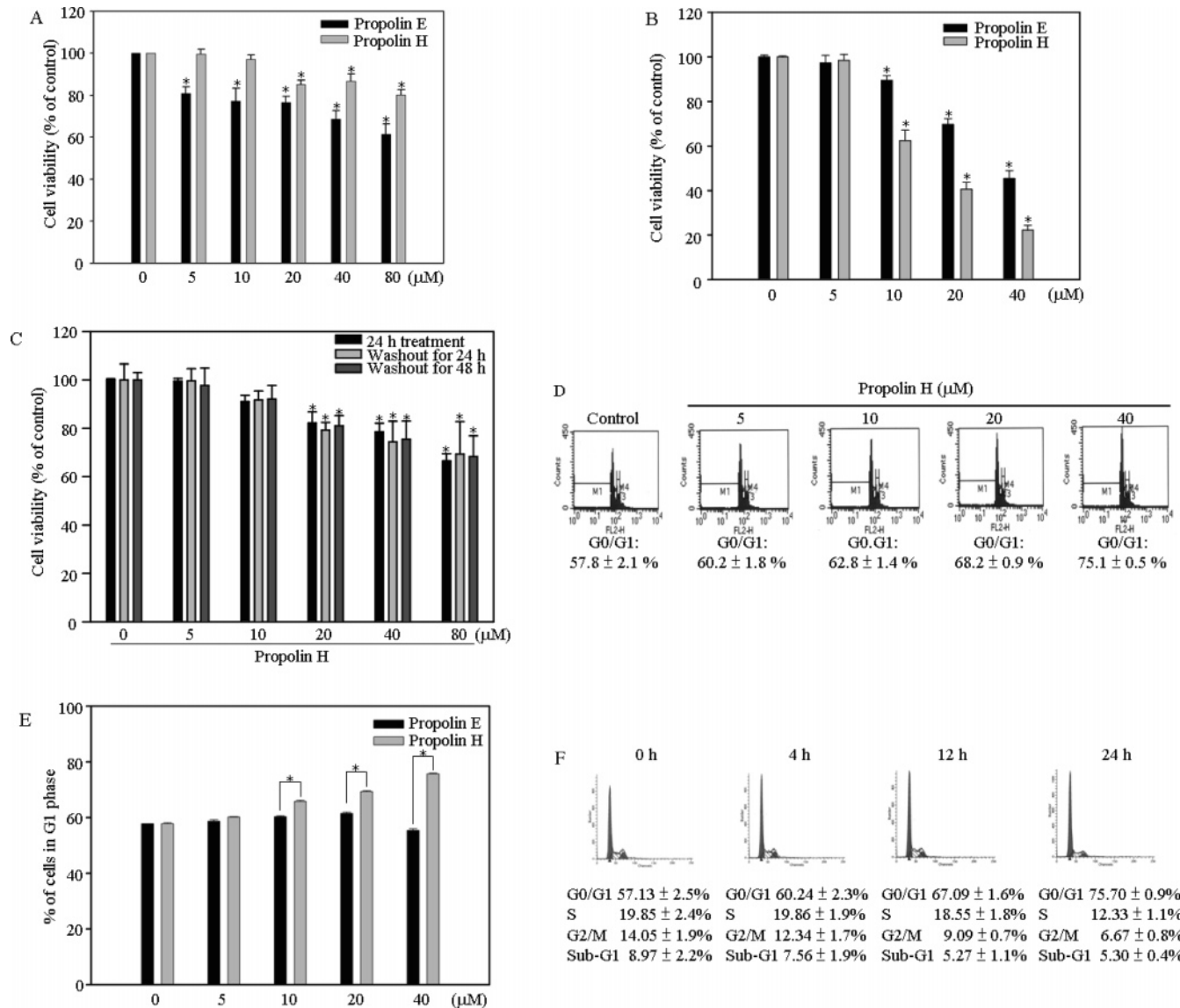


**Figure 2.** Growth inhibitory effects of propolin H on lung carcinoma H460 cells. Dose-dependent inhibition of cell viability was observed in (A) lung carcinoma H460 and (B) human A2058 melanoma cells treated with various concentrations of propolin E and propolin H. Lung carcinoma H460 and human A2058 melanoma cells were maintained in 96 well plates at a density of  $1 \times 10^4$  cells/well for 24 h. Cells were treated with propolin E or propolin H at a dose of 0, 5, 10, 20, 40, and 80  $\mu$ M for 24 h. The MTT assay was performed as described in the Materials and Methods. The percentage of viable cells was calculated as a ratio of  $A_{490\text{nm}}$  of treated cells vs control cells (treated with 0.1% DMSO vehicle). (C) Reversibility of the propolin H-induced inhibition of cell viability. Propolin H-induced inhibition of cell viability was not reversed by removal of propolin H. The H460 cells were incubated in culture media supplemented with 10% serum and 0.1% DMSO without or with various doses of propolin H (0, 10, 20, 40, and 80  $\mu$ M) for 24 h. After 24 h of treatment with propolin H, the cells were washed twice with PBS and replaced with fresh 10% serum without DMSO or propolin H. The propolin H-induced inhibition of cell viability was sustained for at least 48 h after removal of propolin H. (D) Effects of propolin H on cell cycle distribution. H460 cells were treated for 24 h with 0, 5, 10, 20, and 40  $\mu$ M and subjected to flow cytometry analysis for the distribution of cells in the cell cycle as described in the Materials and Methods. (E) Effects of propolin E and propolin H on G1 phase cell cycle distribution. Cells were treated with propolin E or propolin H and flow cytometry analysis for the G1 phase cell cycle distribution. (F) Time-dependent induction of G1 cell cycle in propolin H-treated H460 cells. Cells were treated with 40  $\mu$ M propolin H for indicated times (0, 4, 12, and 24 h), and cell cycle analysis was performed as described in the Materials and Methods. Three samples were analyzed in each group, and values represent the means  $\pm$  SE. Significance was accepted at  $p < 0.05$ . The symbol (\*) indicates that the propolin H-treated group is different from control group.

The p21<sup>Waf1/Cip1</sup> belongs to the Cip/Kip family of endogenous CDK inhibitors, which regulate CDKs activity through direct binding (3, 5, 6). To examine whether propolin H inhibited CDK2 and CDK4 kinase activities through the association between p21<sup>Waf1/Cip1</sup> and CDK2 or CDK4, H460 cells were synchronized by serum-free medium for 24 h and then serum-supplemented medium containing DMSO or 40  $\mu$ M propolin H for 24 h. After 24 h of incubation, cell lysates were immunoprecipitated by CDK2 or CDK4 antibodies and then

immunoblotted by anti-p21<sup>Waf1/Cip1</sup> antibody. As shown in Figure 4B, the levels of CDK2-p21<sup>Waf1/Cip1</sup> and CDK4-p21<sup>Waf1/Cip1</sup> complexes increased after propolin H had been administered for 24 h in H460 cells. Densitometric analysis showed 1.6-fold increases in the bound protein levels of p21<sup>Waf1/Cip1</sup> with CDK2 as compared with control. Meanwhile, the bound levels of p21<sup>Waf1/Cip1</sup> with CDK4 increases were 1.4-fold as compared with control.

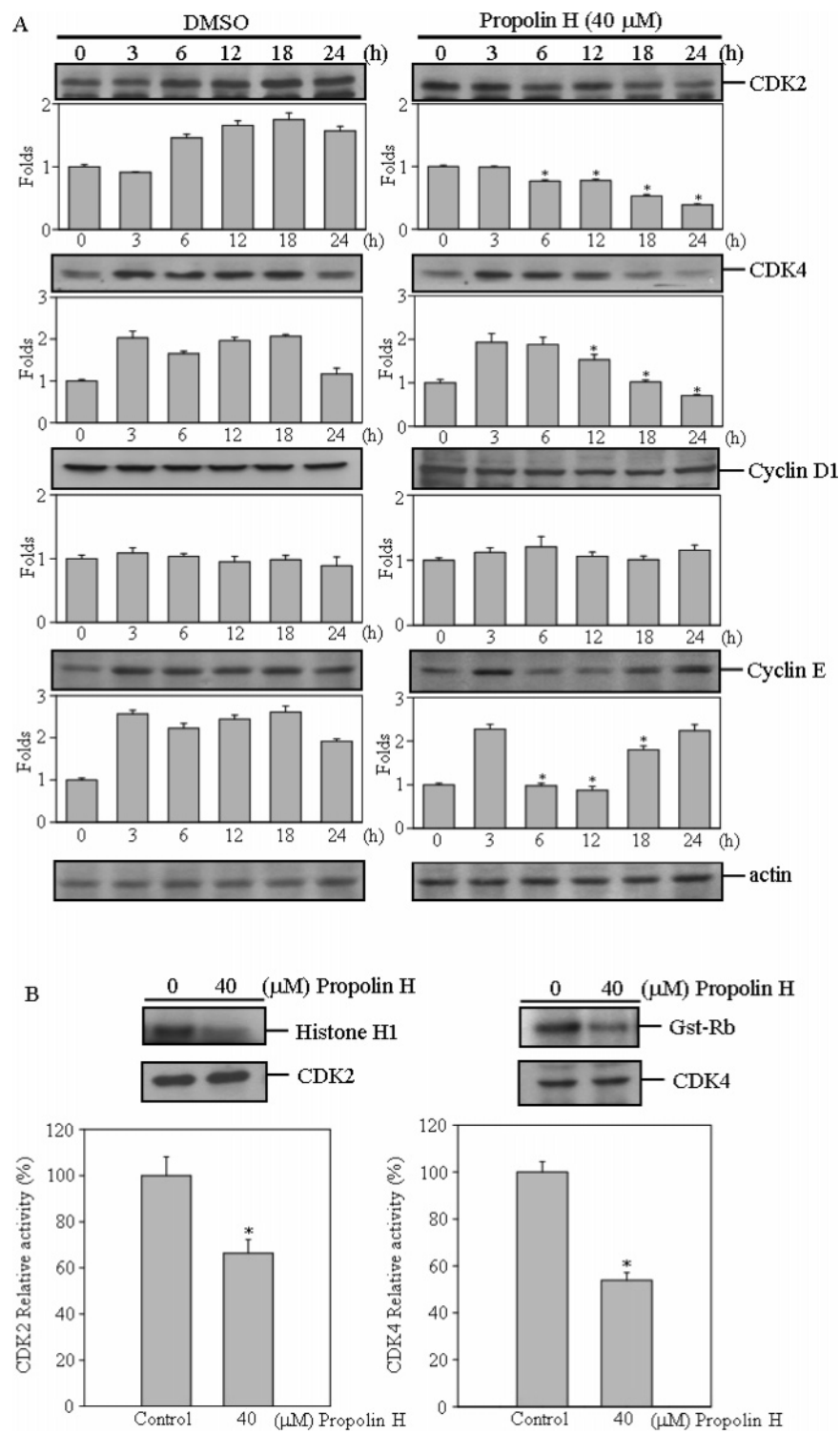


**Figure 3.** Effects of propolin H on the protein levels of cyclins, and CDKs and kinase activities of CDKs in lung carcinoma H460 cells. **(A)** Effects of propolin on the expression of cyclin D1, E, CDK2, and CDK4 in lung carcinoma H460 cells. The H460 cells were synchronized by serum-free medium for 24 h and then serum-supplemented medium containing DMSO or 40  $\mu$ M propolin H for various time points (0, 3, 6, 12, 18, and 24 h). After the cells were harvested, western blot analyses were done with anti-cyclin D1, cyclin E, CDK2, CDK4, and  $\beta$ -actin antibodies as described in the Materials and Methods. Results from a representative experiment are shown. The bottom panel of each band indicates the fold change in band intensity as compared with that of 0 h at each treatment time. **(B)** Effects of propolin H on the kinase activities of CDK2 and CDK4 in cell-free system. H460 cells were synchronized by serum-free medium for 24 h and then serum-supplemented medium containing DMSO or 40  $\mu$ M propolin H for 24 h. After 24 h, cells were harvested for immunoprecipitation, and kinase activities were performed as described in the Materials and Methods. The kinase activities associated with CDK2 immunocomplexes were analyzed with histone H1, and CDK4 was analyzed with G1-Rb as the substrate. CDK2 and CDK4 levels were used as loading controls. The kinase activities in each treatment normalized with the levels of immunoprecipitation loading control are shown. Three samples were analyzed in each group, and values represent the means  $\pm$  SE. Significance was accepted at  $p < 0.05$ . The symbol (\*) indicates that the propolin H-treated group is different from the control group.

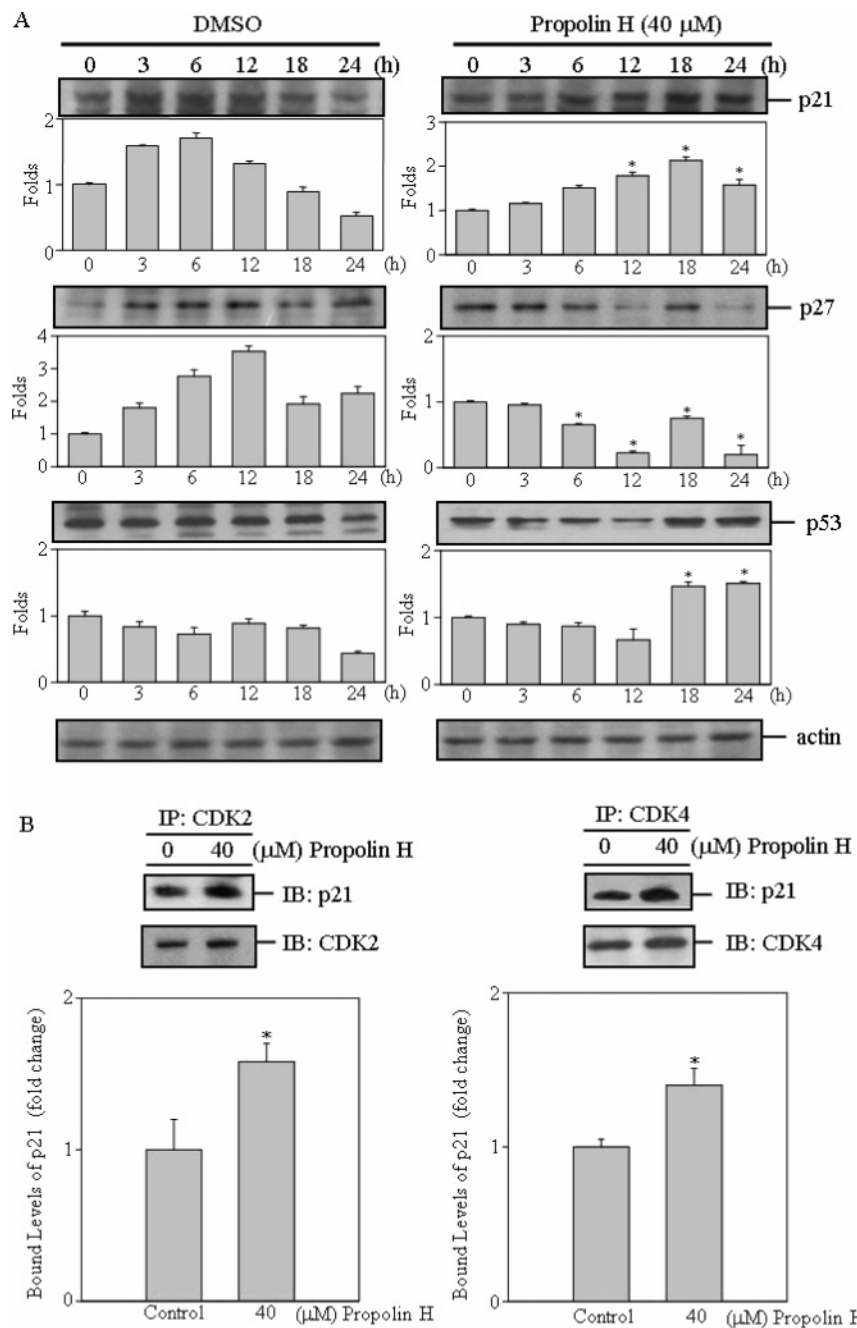


**Figure 4.** Effects of propolin H on the expression of CDK1 and p53, and CDKs-CDK1 complex in lung carcinoma H460 cells. **(A)** Effects of propolin on the expression of p21<sup>Waf1/Cip1</sup>, p27<sup>Kip1</sup>, and p53 in lung carcinoma H460 cells. H460 cells were synchronized by serum-free medium for 24 h and then serum-supplemented medium containing DMSO or 40  $\mu$ M propolin H for various time points (0, 3, 6, 12, 18, and 24 h). After the cells were harvested, western blot analyses were done with anti-p21<sup>Waf1/Cip1</sup>, p27<sup>Kip1</sup>, p53, and  $\beta$ -actin as described in the Materials and Methods. **(B)** Effects of propolin H on the formation of CDK2-p21<sup>Waf1/Cip1</sup> and CDK4-p21<sup>Waf1/Cip1</sup> complexes. Cells were treated with 40  $\mu$ M propolin H for 24 h and immunoprecipitated with anti-CDK2 or CDK4 as described in the Materials and Methods. Western blot analysis was done with anti-p21<sup>Waf1/Cip1</sup> antibody. CDK2 and CDK4 levels were used as loading controls. The bound levels of p21<sup>Waf1/Cip1</sup> in each treatment normalized with the levels of immunoprecipitation loading control are shown. Three samples were analyzed in each group, and values represent the means  $\pm$  SE. Significance was accepted at  $p < 0.05$ . The symbol (\*) indicates that the propolin H-treated group is different from the control group.

**Propolin H-Induced G1 Cell Cycle Arrest through a p53-Independent Mechanism.** The p53 protein has been suggested to be a potent transcription factor involved in the regulation of cell cycle arrest and occurrence of apoptosis (9, 11, 25–27). **Figure 4A** showed that the levels of p21<sup>Waf1/Cip1</sup> and p53 protein increased in a time-dependent manner in propolin H-treated H460 cells. This data suggested that G1 arrest induced by propolin H in H460 cells may be mediated through the up-regulation of p53 and p21<sup>Waf1/Cip1</sup> protein. To further confirm this hypothesis, we examined the effects of propolin H in

regulation of cell cycle in p53-mutant and p53-null lung cancer cell lines, H1155 and H1299, respectively. The H1155 (p53-mutant) and H1299 (p53-null) were cultured in complete medium for 24 h and then treated with propolin H at various concentrations (5, 10, 20, and 40  $\mu$ M) for 24 h. The cell viability was determined by MTT assay, and then, a dose-dependent inhibition of cell proliferation was observed both in H1155 and in H1299 cells. As shown in **Figure 5A**, the amount of 40  $\mu$ M propolin H-treated H1155 and H1299 cells fell by approximately 55 and 58.4%, respectively. To further determine the antipro-

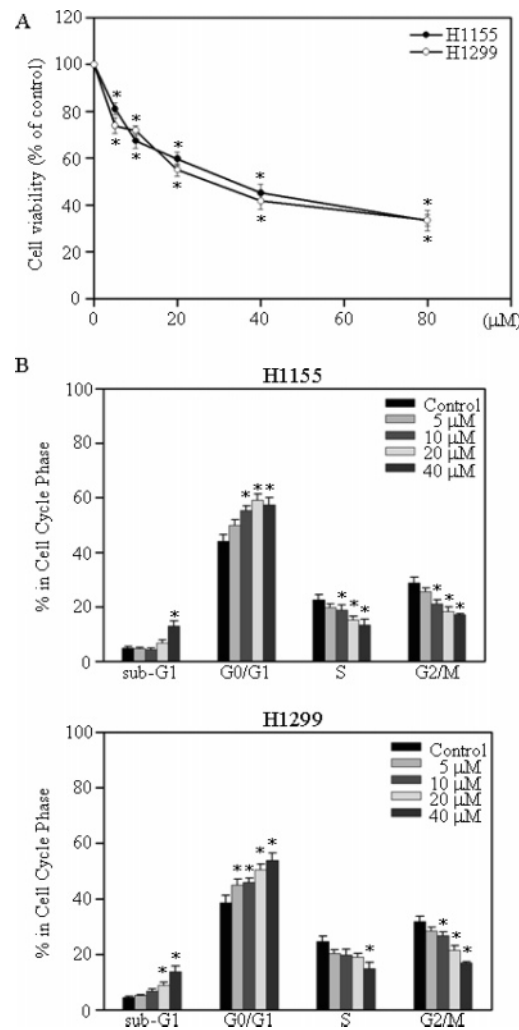


**Figure 5.** Effects of propolin H on p53-mutant H1155 and p53-null H1299 lung carcinoma cells. (A) Effects of propolin H on cell viability of p53-mutant H1155 and p53-null H1299 lung carcinoma cells. Cells were cultured in complete medium in 96 well plates at a density of  $1 \times 10^4$  cells/well for 24 h. Then, cells were treated with propolin H at doses of 0, 5, 10, 20, 40, and 80  $\mu$ M for 24 h. The MTT assay was performed as described in the Materials and Methods. (B) Effects of propolin H on the cell cycle distribution of p53-mutant H1155 and p53-null H1299 lung carcinoma cells. Cells were synchronized with serum-free medium for 24 h as described in the Materials and Methods. After they were synchronized, the cells were released into complete medium (10% serum) containing 0.1% DMSO or a different concentration of propolin H (0, 5, 10, 20, and 40  $\mu$ M) for 24 h. After 24 h of treatment, cells were harvested for cell cycle distribution analysis. Three samples were analyzed in each group, and values represent the means  $\pm$  SE. Significance was accepted at  $p < 0.05$ . The symbol (\*) indicates that the propolin H-treated group is different from the control group.

liferation efficacy of propolin H in H1155 and H1299 cells, these cells were synchronized by RPMI-1640 medium and then treated with serum-supplemented medium containing various concentrations of propolin H (5, 10, 20, 40, and 80  $\mu$ M) for 24 h. After 24 h of treatment, cells were harvested, and flow cytometry analyses were performed. As shown in **Figure 5B**, both H1155 and H1299 cells treated with propolin H experienced a decrease in the G2/M and S phase cells. The inhibitory effect was accompanied with an increase in G1 and sub-G1 populations relative to control cultures. Propolin H-treated (40  $\mu$ M) H1155 cells undergoing G1 arrest accounted for 44.07–

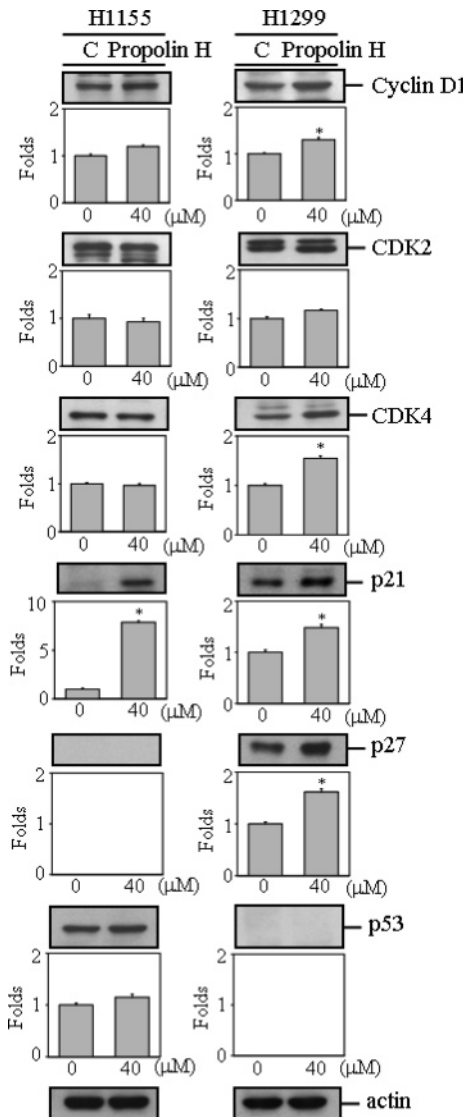


**Figure 6.** Effects of propolin H on the expression of cyclin D1, CDKs, and CDK inhibitors. Cells were treated with DMSO or 40  $\mu$ M propolin H, and western blot was done with anti-cyclin D1, CDK2, CDK4, p21<sup>Waf1/Cip1</sup>, p27<sup>Kip1</sup>, and p53 antibodies as described in the Materials and Methods. Results from a representative experiment are shown.

57.41% of total cells for 24 h of treatment. Apoptotic cells made up 4.96–12.9%. In H1299 cells, treatment with 40  $\mu$ M propolin H increased the proportion of cells in the G1 and sub-G1 phase to 38.68–53.92 and 4.45–13.85%, respectively. To elucidate the specific regulatory proteins responsible for the cell cycle block by propolin H in H1155 and H1299 cells, cell extracts were prepared and western blot analyses were done with anti-cyclin D1, CDKs (CDK2 and CDK4), CDK inhibitors (p21<sup>Waf1/Cip1</sup> and p27<sup>Kip1</sup>), and p53 antibodies, respectively. As shown in **Figure 6**, propolin H treatment caused an increase in cyclin D1 expression in H1299 but not H1155 cells. However, no detectable changes were observed in CDK2 protein levels in either H1155 or H1299 cells. The protein levels of CDK4 were up-regulated after propolin H treatment in H1299 cells, but no significant changes were apparent in H1155 cells. Levels of the CDK inhibitor p21<sup>Waf1/Cip1</sup> also markedly increased with 40  $\mu$ M propolin H treatment in both H1155 and H1299 cells. Another CDK inhibitor, p27<sup>Kip1</sup>, showed enhancement after propolin H treatment in H1299 cells, but H1155 showed none (**Figure 6**). Our data suggested that propolin H-induced G1 cell cycle arrest

also occurs through p53-independent up-regulated p21<sup>Waf1/Cip1</sup> expression in H1155 (p53-mutant) and H1299 (p53-null) lung cancer cells.

## DISCUSSION

In this study, we show that propolin H, isolated from Taiwanese propolis, suppressed cell proliferation through induction of G1 phase cell cycle arrest in H460 cells. Our data displayed that propolin H decreased the expression of CDK2, CDK4, and cyclin D1 proteins. Propolin H also up-regulated p53/p21<sup>Waf1/Cip1</sup> signaling and p21<sup>Waf1/Cip1</sup>, which was associated with CDK2 and CDK4 followed by inhibition of their kinase activities. Furthermore, we demonstrated that propolin H induced the expression of p21<sup>Waf1/Cip1</sup> mediated by an unknown p53-independent pathway and then induced of G1 phase cell cycle arrest and apoptosis in p53-null H1299 and p53-mutant H1155 cells.

Propolis is a folk medicine used for the treatment of various ailments and has been demonstrated to have a broad spectrum of activities (12–17). In our previous work, six prenylflavanone compounds were isolated and characterized from Taiwanese propolis—namely, propolins A, B, C, D, E, and F (Figure 1) (23). In this study, we further isolated and characterized a new component from Taiwanese propolis named propolin H, and we found it to be the functional isomer of propolin E. Propolin E has a hydrated geranyl side chain, whereas propolin H is dehydrated in the geranyl side chain on the B ring at C-3. Both propolin E and propolin H inhibited cell proliferation significantly in human A2058 melanoma cells, with propolin H being even more potent (Figure 2B). This result was consistent with the conclusions of our recent study that propolins with dehydrated geranyl side chains were more effective against cell proliferation than those with hydrated geranyl side chains in human melanoma cells (21–23). Nevertheless, propolin E inhibited cell viability more effectively than propolin H in lung carcinoma H460 cells. Flow cytometric analysis indicated that propolin H induced cell cycle G1 phase arrest in lung carcinoma H460 cells but not apoptosis (Figure 2C). Our data implicate that propolin H induced G1 phase arrest more effectively in contrast with propolin E (Figure 2E).

Cell cycle control is a highly regulated process that involves a complex cascade of events. Modulation of the expression and function of the cell cycle regulatory proteins (including cyclins, CDKs, and CDKIs) provides an important mechanism for inhibition of growth (1–6). In the present study, we showed that propolin H down-regulated the expression of CDK2 and CDK4 in a time-dependent manner (Figure 3A) and strongly inhibited their kinase activities (Figure 3B). The inhibition of kinase activities of CDK2 and CDK4 by propolin H may facilitate cell cycle blocking in the G1 phase in H460 lung carcinoma cells. The physiological roles of CDK inhibitors, p21<sup>Waf1/Cip1</sup> and p27<sup>Kip1</sup>, have been linked to the inhibition of G1-related CDKs kinase activities (3, 5, 6, 8). In our study, a marked increase in the protein levels of p21<sup>Waf1/Cip1</sup> and p53 was detected in propolin H-treated H460 cells in a time-dependent manner while the level of p27<sup>Kip1</sup> protein decreased (Figure 4A). These data suggested that p53 may play an essential but not the exclusive role to regulate the expression of p21<sup>Waf1/Cip1</sup>. Furthermore, immunoprecipitation Western analysis showed that the formation of CDK2-p21<sup>Waf1/Cip1</sup> and CDK4-p21<sup>Waf1/Cip1</sup> complexes increased in propolin H-treated H460 cells (Figure 4B). These results suggested that propolin H induced the expression of p21<sup>Waf1/Cip1</sup>, which was associated with CDK2 and CDK4, and inhibited their kinase activities

followed by induction of G1 phase arrest through a p53-dependent pathway in H460 lung carcinoma cells.

The p53 protein is the most extensively studied tumor suppressor and acts in response to diverse forms of cellular stress to mediate a variety of antiproliferative processes (11, 25–27). However, mutations in the *p53* gene have been identified with high frequencies in both NSCLC and SCLC, with mutation frequencies of 50 and 70%, respectively. Mutations of the *p53* gene comprise some of the most common genetic changes associated with cancer and cause loss of tumor suppressor function and loss of the ability to induce apoptotic cell death. Numerous reports have investigated the association of *p53* abnormalities with the prognosis of NSCLC patients; nonetheless, all results were inconclusive (28–30). Thus, p53 has been introduced into clinical trials with retroviral and adenoviral gene therapy delivered directly into tumors with initially promising antitumor responses (31). Pharmacological agents that specifically activate p53-dependent cell cycle control and cell death pathways in mutant p53-accumulating cancer cells would represent a major advance in the therapy of human cancers characterized by p53 mutations. In the present study, we also examined the effects of propolin H in p53-mutant H1155 and p53-null H1299 lung carcinoma cells. Figure 5 showed that propolin H induced cell cycle G1 arrest and apoptosis in p53-mutant H1155 and p53-null H1299 lung carcinoma cells. Western blot analysis indicated that propolin H profoundly up-regulated the expression of p21<sup>Waf1/Cip1</sup> in both H1155 and H1299 cells and p27<sup>Kip1</sup> in H1299 cells (Figure 6). These data suggest that propolin H induced the expression of p21<sup>Waf1/Cip1</sup> through an unidentified p53-independent pathway followed by induction cell cycle arrest in the G1 phase in p53-mutant and p53-null lung carcinoma cells. A recent study has demonstrated that the PKC- and MAPK-mediated signaling pathway has been suggested to be involved in the regulation of p21<sup>Waf1/Cip1</sup> expression (32, 33). On the basis of this study, propolin H may induce a PKC- or MAPK-mediated signaling pathway and then mediate cell cycle arrest. Otherwise, H1299 p53-null cells and H1155 p53-mutant cells may be due to some residual p53 activity as well as to effects of propolin H on other members of the p53 family, such as p63 or p73.

In summary, we have demonstrated that exposure of various NSCLC cell lines to propolin H results in G1 arrest and induction of apoptosis. The growth inhibitory action of propolin H appears to involve the up-regulation of the p53/p21<sup>Waf1/Cip1</sup> pathway following inhibition of the kinase activities of CDK2 and CDK4. Moreover, propolin H also induced the expression of p21<sup>Waf1/Cip1</sup> and p27<sup>Kip1</sup> through a p53-independent pathway and consequently induced cell cycle arrest in the G1 phase in p53-mutant and p53-null lung carcinoma cells.

## LITERATURE CITED

- (1) Malumbres, M.; Barbacid, M. To cycle or not to cycle: A critical decision in cancer. *Nat. Rev. Cancer* **2001**, *1*, 222–231.
- (2) Sherr, C. J. Cancer cell cycles. *Science* **1996**, *274*, 1672–1677.
- (3) Morgan, D. O. Principles of CDK regulation. *Nature* **1995**, *374*, 131–134.
- (4) Pines, J. Cyclins: Wheels within wheels. *Cell Growth Differ.* **1991**, *2*, 305–310.
- (5) Sherr, C. J.; Roberts, J. M. Inhibitors of mammalian G1 cyclin-dependent kinases. *Genes Dev.* **1995**, *9*, 1149–1163.
- (6) Pietenpol, J. A.; Stewart, Z. A. Cell cycle checkpoint signaling: Cell cycle arrest versus apoptosis. *Toxicology* **2002**, *181–182*, 475–481.
- (7) Dyson, N. The regulation of E2F by pRB-family proteins. *Genes Dev.* **1998**, *12*, 2245–2262.

- (8) Liu, G.; Lozano, G. p21 stability: Linking chaperones to a cell cycle checkpoint. *Cancer Cell* **2005**, *7*, 113–114.
- (9) Levine, A. J. p53, the cellular gatekeeper for growth and division. *Cell* **1997**, *88*, 323–331.
- (10) Mittnacht, S. Control of pRB phosphorylation. *Curr. Opin. Genet. Dev.* **1998**, *8*, 21–27.
- (11) Lane, D. P.; Lain, S. Therapeutic exploitation of the p53 pathway. *Trends Mol. Med.* **2002**, *8*, S38–S42.
- (12) Burdock, G. A. Review of the biological properties and toxicity of bee propolis. *Food Chem. Toxicol.* **1998**, *36*, 347–363.
- (13) Gekker, G.; Hu, S.; Spivak, M.; Lokensgaard, J. R.; Peterson, P. K. Anti-HIV-1 activity of propolis in CD4(+) lymphocyte and microglial cell cultures. *J. Ethnopharmacol.* **2005**, *102*, 158–163.
- (14) Banskota, A. H.; Tezuka, Y.; Kadota, S. Recent progress in pharmacological research of propolis. *Phytother. Res.* **2001**, *15*, 561–571.
- (15) Sonmez, S.; Kirilmaz, L.; Yucesoy, M.; Yucel, B.; Yilmaz, B. The effect of bee propolis on oral pathogens and human gingival fibroblasts. *J. Ethnopharmacol.* **2005**, *102*, 371–376.
- (16) Khalil, M. L. Biological activity of bee propolis in health and disease. *Asian Pac. J. Cancer Prev.* **2006**, *7*, 22–31.
- (17) Liu, C. F.; Lin, C. H.; Lin, C. C.; Lin, Y. H.; Chen, C. F.; Lin, S. C. Protective effect of propolis ethanol extract on ethanol-induced renal toxicity: An in-vivo study. *Am. J. Chin. Med.* **2005**, *33*, 779–786.
- (18) Bankova, V.; Christov, R.; Kujumgiev, A.; Marcucci, M. C.; Popov, S. Chemical composition and antibacterial activity of Brazilian propolis. *Z. Naturforsch., C: J. Biosci.* **1995**, *50*, 167–172.
- (19) Christov, R.; Trusheva, B.; Popova, M.; Bankova, V.; Bertrand, M. Chemical composition of propolis from Canada, its antiradical activity and plant origin. *Nat. Prod. Res.* **2006**, *20*, 531–536.
- (20) Trusheva, B.; Popova, M.; Bankova, V.; Simova, S.; Marcucci, M. C.; Miorin, P. L.; da Rocha Pasin, F.; Tsvetkova, I. Bioactive constituents of brazilian red propolis. *Evidence Based Complement Alternat. Med.* **2006**, *3*, 249–254.
- (21) Chen, C. N.; Wu, C. L.; Lin, J. K. Propolin C from propolis induces apoptosis through activating caspases, Bid and cytochrome c release in human melanoma cells. *Biochem. Pharmacol.* **2003**, *67*, 53–66.
- (22) Chen, C. N.; Wu, C. L.; Shy, H. S.; Lin, J. K. Cytotoxic prenylflavanones from Taiwanese propolis. *J. Nat. Prod.* **2003**, *66*, 503–506.
- (23) Chen, C. N.; Weng, M. S.; Wu, C. L.; Lin, J. K. Comparison of radical scavenging activity, cytotoxic effects and apoptosis induction in human melanoma cells by Taiwanese propolis from different source. *Evidence Based Complement Alternat. Med.* **2004**, *1*, 175–185.
- (24) Chen, C. N.; Wu, C. L.; Lin, J. K. Apoptosis of human melanoma cells induced by the novel compounds propolin A and propolin B from Taiwanese propolis. *Cancer Lett.* **2007**, *245*, 218–231.
- (25) Eastman, A. Cell cycle checkpoints and their impact on anticancer therapeutic strategies. *J. Cell. Biochem.* **2004**, *91*, 223–231.
- (26) Giaccia, A. J.; Kastan, M. B. The complexity of p53 modulation: Emerging patterns from divergent signals. *Genes Dev.* **1998**, *12*, 2973–2983.
- (27) Vousden, K. H.; Lu, X. Live or let die: the cell's response to p53. *Nat. Rev. Cancer* **2002**, *2*, 594–604.
- (28) Mitsudomi, T.; Oyama, T.; Kusano, T.; Osaki, T.; Nakanishi, R.; Shirakusa, T. Mutations of the p53 gene as a predictor of poor prognosis in patients with nonsmall-cell lung cancer. *J. Natl. Cancer Inst.* **1993**, *85*, 2018–2023.
- (29) Kawasaki, M.; Nakanishi, Y.; Kuwano, K.; Yatsunami, J.; Takayama, K.; Hara, N. The utility of p53 immunostaining of transbronchial biopsy specimens of lung cancer: p53 overexpression predicts poor prognosis and chemoresistance in advanced non-small cell lung cancer. *Clin. Cancer Res.* **1997**, *3*, 1195–1200.
- (30) Tomizawa, Y.; Kohno, T.; Fujita, T.; Kiyama, M.; Saito, R.; Noguchi, M.; Matsuno, Y.; Hirohashi, S.; Yamaguchi, N.; Nakajima, T.; Yokota, J. Correlation between the status of the p53 gene and survival in patients with stage I non-small cell lung carcinoma. *Oncogene* **1999**, *18*, 1007–1014.
- (31) Roth, J. A.; Swisher, S. G.; Merritt, J. A.; Lawrence, D. D.; Kemp, B. L.; Carrasco, C. H.; El-Naggar, A. K.; Fossella, F. V.; Glisson, B. S.; Hong, W. K.; Khurl, F. R.; Kurie, J. M.; Nesbitt, J. C.; Pisters, K.; Putnam, J. B.; Schrump, D. S.; Shin, D. M.; Walsh, G. L. Gene therapy for non-small cell lung cancer: A preliminary report of a phase I trial of adenoviral p53 gene replacement. *Semin. Oncol.* **1998**, *25*, 33–37.
- (32) Walker, J. L.; Castagnino, P.; Chung, B. M.; Kazanietz, M. G.; Assoian, R. K. Post-transcriptional destabilization of p21cip1 by protein kinase C in fibroblasts. *J. Biol. Chem.* **2006**, *281*, 38127–38132.
- (33) Hsu, Y. L.; Kuo, P. L.; Lin, L. T.; Lin, C. C. Asiatic acid, a triterpene, induces apoptosis and cell cycle arrest through activation of extracellular signal-regulated kinase and p38 mitogen-activated protein kinase pathways in human breast cancer cells. *J. Pharmacol. Exp. Ther.* **2005**, *313*, 333–344.

Received for review January 23, 2007. Revised manuscript received April 12, 2007. Accepted April 12, 2007. This work was supported by Grants NSC-95-2320-B-002-111 and NSC-95-2321-B-002-016 from the National Science Council.

JF070201N